Defects in GaN: Core structure of screw dislocations

Z Liliental-Weber, D Zakharov, J Jasinski, and MA O'Keefe

Lawrence Berkeley National Laboratory, Berkeley, CA 94720 m/s 62/203

ABSTRACT: Screw dislocations in GaN grown by HVPE and MBE have been studied using Transmission Electron Microscopy (TEM). It was shown that screw dislocations in the HVPE layers are decorated by small voids arranged along the screw axis, but voids were not observed along screw dislocations in MBE overlayers grown on top of the HVPE layers. A direct reconstruction of the phase and amplitude of the scattered electron wave from a focal series of high-resolution images showed that the core structures of screw dislocations in all studied materials were filled. Dislocation cores in MBE samples were stoichiometric. However, in HVPE materials, single atomic columns show substantial differences in intensities and indicate the possibility of Ga presence.

1. INTRODUCTION

GaN has received much attention over the past few years because of several new applications, including light emitting diodes, blue laser diodes (Nakamura et al., 1998) and high-power microwave transistors (Trew et al., 1997). One of the biggest problems of this material is the high density of structural defects, mostly dislocations, due to a lack of a suitable lattice-matched substrate. Al_2O_3 substrates usually are used for the heteroepitaxial growth of (0001) GaN. This leads to high concentrations (typically 10^9-10^{11} cm^{-2}) of threading edge, screw and mixed dislocations that propagate vertically from the GaN/Al_2O_3 interface to the GaN surface (Heying et al., 1996; Ponce et al., 1996). Nanotubes and pinholes are other types of defects present in this material (Liliental-Weber et al., 1997a; 1997b). These defects are empty areas (voids), which either extend along the growth direction (tubes), or form V-shape defects on (10$\underline{1}$1) planes (pinholes), with hexagonal shaped bases along the c-plane. In most cases, nanotubes and pinholes are formed close to the dislocations, but in some cases these defects are formed in dislocation free areas. The density of these defects was estimated to be in the range of 10^5 -10^7 cm^{-2} and their radii in the range 3–1500 nm. It was suggested (Liliental-Weber et al., 1997a; 1997b) that these two types of defects are related to the presence of impurities in the material, supporting theoretical work by Elsner et al., (1998), who showed that O and O-related defect complexes can be formed on the walls of nanotubes in GaN.

Despite this high density of dislocations (and other defects), a high emission efficiency has been achieved in optical devices such as light-emitting diodes (LEDs) and laser diodes (LDs) (Nakamura et al., 1998). The most common explanation for this phenomenon is that the threading dislocations in GaN do not have electronic states in the band gap. However, this is still a controversial issue, and there is no agreement on this subject between different scientific groups. There are also discrepancies concerning the nature of dislocation cores in GaN. Some investigators claim that GaN dislocations have open cores (Qian et al.,1995; Elsner et al., 1997) but others suggest that screw dislocations have filled cores (Arslan & Browning, 2002). First-principles total energy calculations showed Ga-filled screw dislocation cores to be stable in Ga-rich growth conditions (Northrup, 2001 and 2002).

2. EXPERIMENTAL

Screw dislocations have been studied in GaN grown by different growth methods: Hydride Vapor Phase Epitaxy (HVPE) and Molecular Beam Epitaxy (MBE). MBE samples were grown using Ga-rich and Ga-lean conditions. Transmission Electron Microscopy (TEM) has been applied to study these layers in electron-transparent samples in plan-view and cross-section. Determination of dislocation core structure from plan-view samples was carried out using a modified 300keV field emission Philips electron microscope (OÅM-CM300FEBG/UT) (O'Keefe et al 2001) to obtain high

resolution focal series with a constant defocus step. The electron exit wave from the crystal structure was obtained by numerical reconstruction from the full focal series of 20 images (Thust et al., 1996, Coene et al., 1996).

3. RESULTS AND DISCUSSION

3.1. Defects in the HVPE Grown Layers

Transmission Electron Microscopy (TEM) has been applied to study HVPE layers in plan-view and cross-section samples using 002B Topcon microscope (200keV) and a modified Phillips microscope, mentioned above. The density of dislocations close to the sample surface of a 1μm-thick HVPE sample was in the range of $3x10^9 cm^{-2}$. All three types of dislocations were present in these samples, with almost 50% screw dislocations (Figs. 1a and 1b). When the diffraction condition **g.b**=0 was applied in cross-section samples and screw dislocations were out of contrast, small voids (pinholes) were observed along screw dislocations (Figs. 1c and 1d).

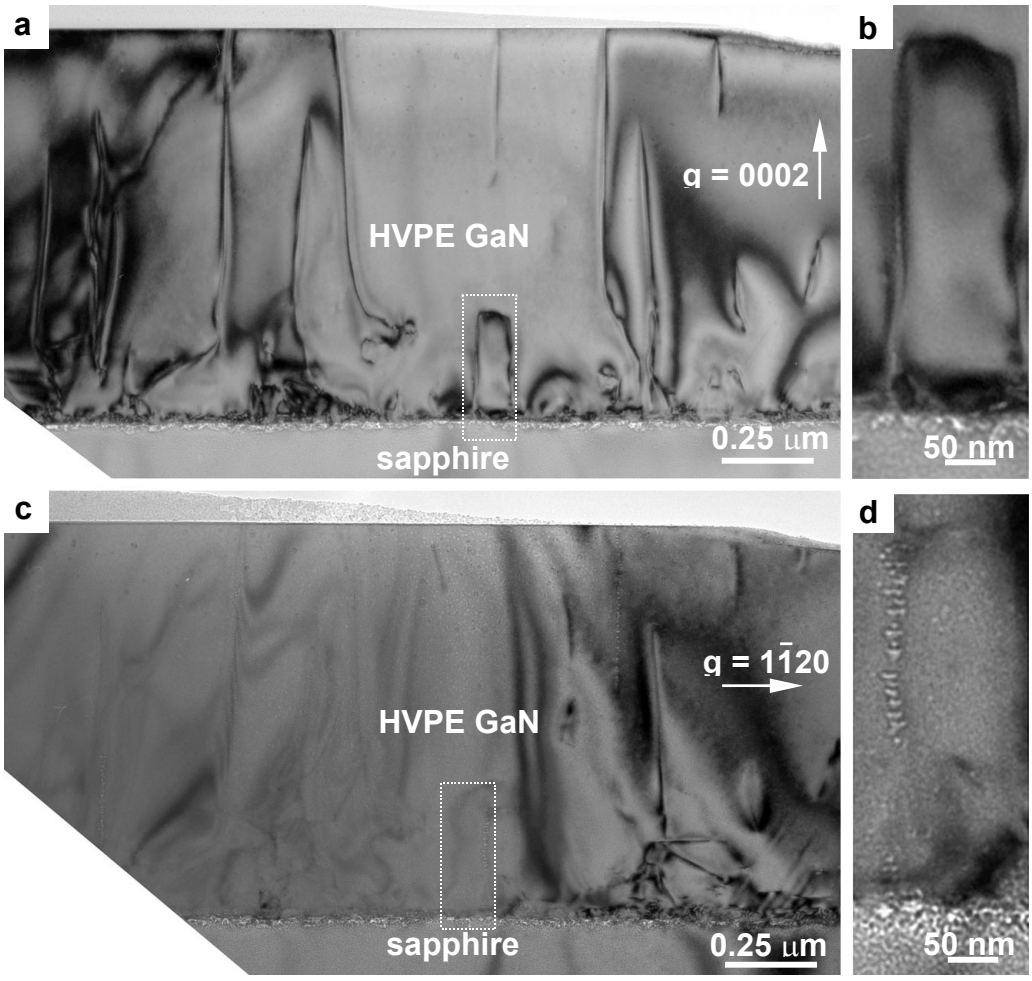

Fig. 1. Cross-section images of HVPE-grown material; a) screw dislocations are in contrast for g=(0002), outlined screw dislocation shown in higher magnification in (b); c) the same image as in (a) for **g**=(11$\underline{2}$0)). Magnified image of the outlined dislocation is shown in (d). Note voids stacked vertically decorating screw dislocation.

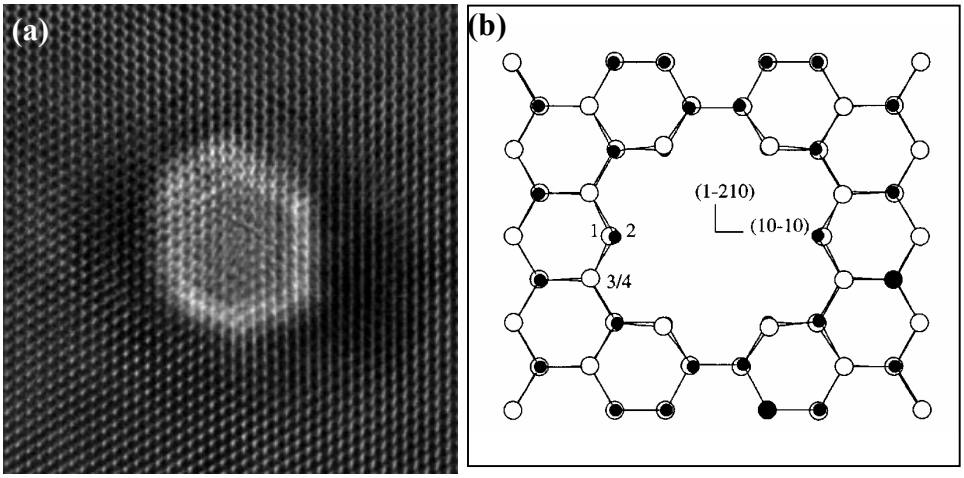

Fig. 2. (a) Plan view image of screw dislocation in HVPE grown GaN. Light contract is due to a void (a pinhole) formed along the dislocation line (smaller thickness and the possibility of light elements like oxygen present there; (b) A model of a screw dislocation with an open core proposed by Elsner et al., (1997).

In the [11$\underline{2}$0] projection, these voids had a triangular shape with a base size of 3 nm and a height of about 4 nm. The voids were arranged tip to base on top of each other, with the direction from the tip to the base along the Ga to N bond length parallel to the c-axis (Ga polarity). Small gaps could be observed between these voids (Fig. 1d). In plan-view configuration the voids had a hexagonal shape (Fig. 2a). In some cases, by changing the defocus, one can reach the tip of the void and observe crystallographic planes around and below the void (Fig. 2a). Voids were not observed along edge dislocations in the same sample. Along some of the screw dislocations, nanotubes that are also empty inside were observed (not shown in this work). We observed earlier similar voids in MOCVD material (Liliental-Weber, et al., 1997a) and suggested that the reason for their formation can be contamination – most probably by oxygen. Theoretical predictions (Elsner et al., 1998) confirmed our suggestion and showed the possibility of V_{Ga}-$(O_N)_3$ pair formation along particular crystallographic planes. When such complexes are formed, the GaN does not grow on these planes, leading to void formation.

The electron exit wave from the crystal structure was obtained by numerical reconstruction (Thust et al., 1996; Coene et al., 1996) from the full focal series of 20 images of dislocation core structure obtained from plan-view samples carried out using a modified 300keV field emission Philips electron microscope (OÅM-CM300FEG/UT). However, screw dislocations have displacements along the c-axis, therefore, continuous tilt of c-planes is expected. For this reason one would need to know how this tilt affects the experimental images. In order to learn how the image changes with the sample tilt and with change of stoichiometry, focal series were simulated using the MacTempas HRTEM image simulation programs (O'Keefe & Kilaas, 1987). The Phillips/Brite-Euram focal-series reconstruction program (Thust et al., 1996; Coene et al., 1996) was then applied to obtain numerical phase and amplitude reconstruction at the sample exit plane.

3.2. Influence of tilt and stoichiometry on the intensity of the atomic columns

Intensity at atomic columns depends strongly on material stoichiometry. Atoms with higher atomic number Z scatter more strongly than those with lower Z, and therefore, produce higher intensity. In order to compare intensity of atomic columns, the same sample thickness should be considered. Larger number of atoms will contribute more to the image, unless sample is too thick and dynamic effects and absorption will attenuate the image intensity. Image simulation for a

stoichiometric screw dislocation shows that the phase of the exit-surface wave changes from white atoms to black atoms for GaN matrix and dislocation core at 80Å (Figs. 3a and 3b). This is an effect of an interaction between primary and diffracted beams, which changes with sample thickness, tilt and sample composition. If a dislocation core is stoichiometric, the position of the core has only slightly larger opening (negligible in an experimental image) between the atomic columns and no change in the columns intensity (see Figs. 3a and 3b). To obtain useful information, the sample thickness needs to be chosen in such a way that all beams contributing to image formation have similar phases and do not attenuate each other. This is especially important when one considers different composition along the dislocation core. When N atoms are removed from the dislocation core as suggested by Northrup (2001) different contrast can be seen within the core and in the matrix for the same sample thickness like 40Å (Fig. 3c). For change of thickness to 80Å matrix atoms change to the black atom image while the core atoms still remain white (Fig. 3d). Additional calculations show that much brighter atom image can be observed when N atoms are substituted by Ga, but such atomic columns would change to black atom image for smaller sample thickness than the surrounding matrix (for details see Liliental-Weber et al., 2003). If dislocation core stoichiometry changes, this would be easy to observe for any sample thickness due to the different contrast of atomic columns in the matrix and in the core.

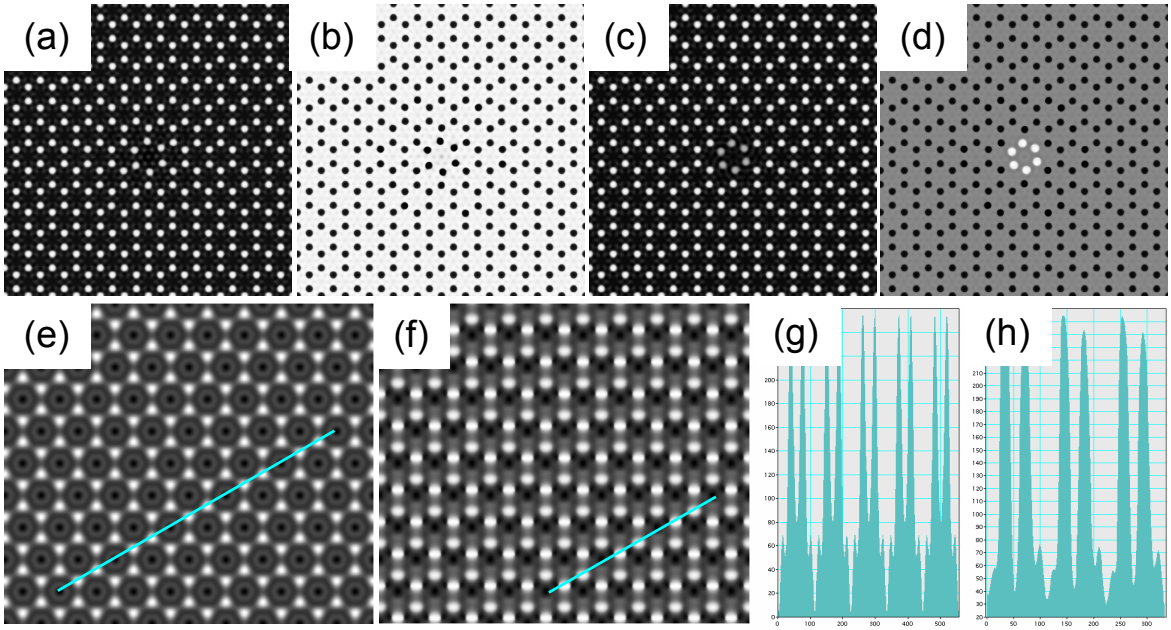

Fig. 3. Simulations of reconstructed phase from dislocation models. For the stoichiometric screw dislocation core the white atom image changes to black atoms on going from a thickness of 40Å (a) to 80Å (b). The calculated Ga-rich dislocation core (N-atoms removed) shows different contrast from the matrix for sample thickness of 45Å (c) and 60Å (d). For the sample thickness of 160Å, images simulated without tilt (e) and with 4 mrad tilt (f) produce symmetric and non-symmetric intensities of atomic columns along (11$\underline{2}$0) planes: without tilt (g) and with tilt (h).

Additional changes are observed when a specimen is tilted. For a 4 mrad tilt along the 0001 axis, a partial change from white atoms to black atoms starts already at a sample thickness of 60Å, and the image changes again to white atoms at a thickness of 140Å (Liliental-Weber et al., 2003). For thin samples in the range of 20Å or 40Å the tilted image preserves six-fold symmetry, but changes to two-fold symmetry for larger sample thickness. If one chooses, for example, the 160Å thick sample then one can observe that pattern symmetry is changing with tilt (Fig. 3e, f) and the atomic columns are no longer round (Fig. 3f). Based on detailed earlier calculations (Liliental-Weber et al., 2003) one can conclude that sample tilt is easy to recognize and thus it can be taken into account in experimental image interpretation. For samples without tilt, each atomic column has the same intensity, and

measurements along specific crystallographic directions (as shown on Fig. 3 e) show the same height (Fig. 3g). However, for small tilts like 4 mrad, due to the symmetry change (Fig. 3f), tracings along the same crystallographic direction show that the intensity changes by 4.5% (Figs. 3h).

3.3. Core of screw dislocation in the HVPE samples

In order to obtain information about dislocation core structures, observations were performed in plan-view configuration. No displacement vector can be observed around screw dislocations in plan-view configuration, since the displacement vector is along the c-axis. As expected from the cross-sectioned samples, voids are observed surrounding the screw dislocation in the HVPE sample. These voids have a hexagonal shape (lighter contrast in the central part of Fig. 2a). To obtain structural information at higher resolution, 20 micrographs were obtained from each screw dislocation at large values of defocus and the complex electron wave was reconstructed numerically (Thust et al., 1996; Coene et al., 1996). An image of the phase of the exit-surface wave gives information on the distribution of atomic columns. Only low-drift images were considered.

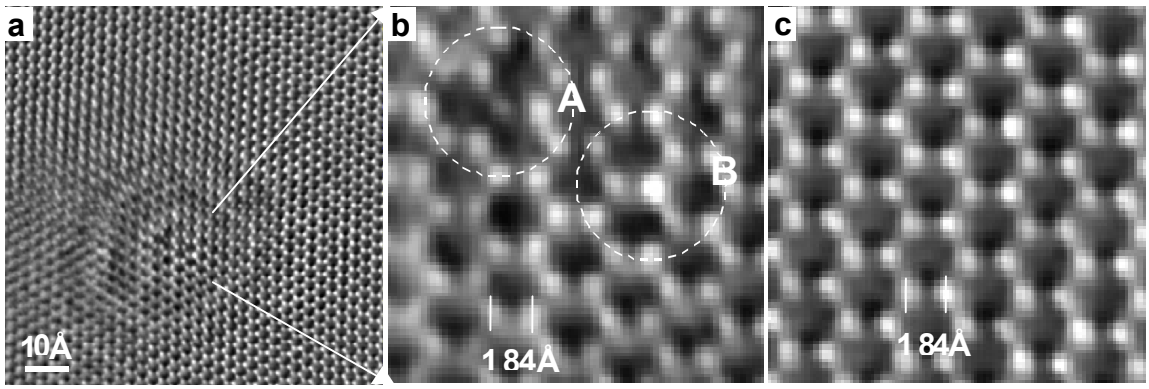

Fig. 4. (a) Phase of the electron wave reconstruction from a screw dislocation surrounded by a void; (b) dislocation core structure – around the tip of the void (circle A) and around the dislocation core (circle B); (c) The perfect area of the matrix observed on the right from the dislocation core. Note the presence of atomic columns within the dislocation core.

We looked for missing atomic columns expected for the empty core model (shown in Fig. 2b) and for changes in intensity of particular columns to indicate the possibly of a nonstoichiometric core. Since the void surrounds the dislocation, such a dislocation might be expected to have an open core. Examination of the intensity of particular columns does not allow us to come to such a conclusion, since all six columns in each cell are present (Figs. 4a and b), similarly as in the matrix (Fig. 4c). Therefore, even in the sample where a screw dislocation is decorated by voids, a screw dislocation has a full core. Careful examination of the intensity of particular atomic columns within the dislocation core shows that one atomic column appears to be very weak (Fig. 4b, column circled by A) and another column is very bright (Fig. 4b- column circled by B). These columns are not adjacent to one other, but separated by about 8 Å. This distance is comparable to that between a dislocation line and the tip of the pyramidal voids observed in cross-section samples. Intensities of the highest-intensity and lowest-intensity atomic columns lie more than three standard deviations from the mean atomic column peak intensity in the matrix. The intensity difference between the highest-intensity and lowest-intensity atomic columns is therefore about six standard deviations. This intensity difference cannot be explained simply by sample tilt, therefore it can be assigned only to the stoichiometry of the particular columns. It is noticeable that the intensity of one column within the core is much brighter than the intensities of other columns, suggesting that this column is heavier than the matrix. Based on our calculations of the possible stoichiometry of dislocation cores (Liliental-Weber et al., 2003) including the model proposed by Northrup (2201, 2002), where a Ga rich core is achieved by removing N atoms (see examples of this calculation on Figs. 3c and d) one can conclude that, rather

than being removed, some N atoms were substituted by Ga, leading in this way to higher column intensity.

3.4. Screw dislocations in MBE grown samples

TEM studies of MBE samples grown under Ga excess conditions in plan-view and cross-section samples showed that the sample surface was covered by small Ga droplets (Fig. 5a) . Some of these droplets could be found inside the layer (Figs. 5b and c). Screw dislocations were present in these samples, but with no special relation between Ga droplets distribution and dislocations, in disagreement with earlier work (Hsu et al., 2001). In Fig. 5a one droplet lies between an edge dislocation and a screw one, which is out of contrast for this diffraction condition. Figs. 5b and c show the droplet at a distance from screw dislocation which is in contrast on Fig. 5c. Samples grown under Ga-lean conditions did not show droplet formation. Neither of these samples showed voids along screw dislocations. Since our earlier studies suggested that voids in GaN are formed due to some impurities present in the material (mostly oxygen), these studies confirm expectation that growth by MBE (or maybe by this specific MBE machine) is much cleaner than growth with the HVPE method.

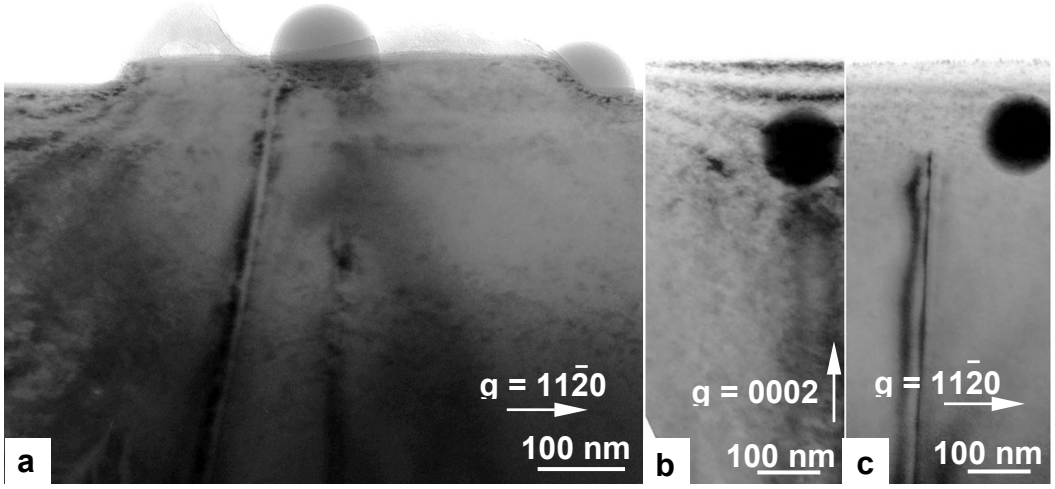

Fig. 5. Cross-section micrographs from the GaN grown by MBE under Ga rich condition. (a) Ga droplets (round balls) on the sample surface and an edge dislocation in contrast; some residual contrast is also observed for a screw dislocation on the right hand side of the central Ga droplet. (b) and (c) show Ga droplet embedded in the GaN layer; a screw dislocation is out of contrast (b) and in contrast (c).

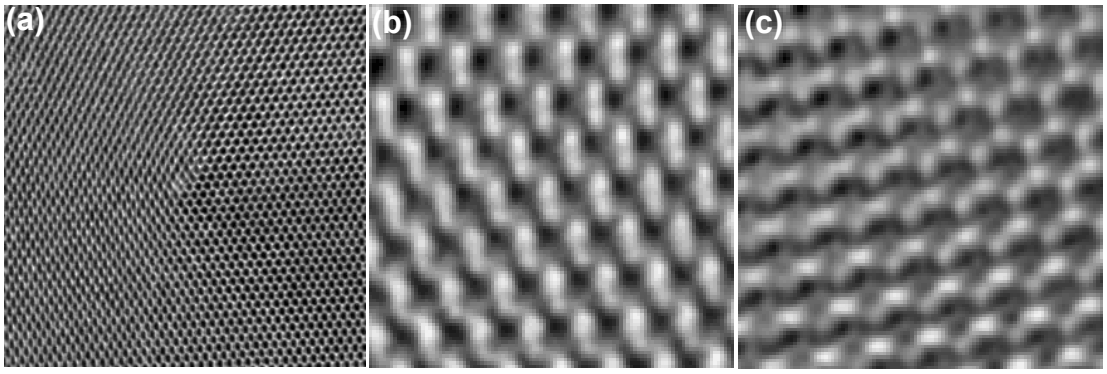

Fig. 6. (a) Screw dislocation in the Ga-rich GaN layer grown by MBE; (b) Reconstructed phase of screw dislocation core in Ga-rich MBE grown GaN and in the Ga-lean GaN (c). Lack of difference in atomic column intensity between center image and surrounding matrix indicates stoichiometric cores.

We again looked for missing atomic columns expected for the empty core model (Fig. 6a), and for changes in intensity of particular columns, to indicate the possibility of a nonstoichiometric core. The focal-series reconstruction technique described above was applied to Ga-rich MBE grown samples in [0001] projection where atomic columns are separated by 1.84Å. No change in intensity between atomic columns can be observed for the Ga rich or Ga-lean samples (Fig. 6b and c), suggesting that dislocation cores studied in these samples were stoichiometric and also have full cores. This result is in agreement with early work of Arslan and Browning (2002).

4. CONCLUSIONS

TEM studies of HVPE and MBE GaN show that core structure of screw dislocations might be different depending on the growth method. In the HVPE grown material screw dislocations are decorated by voids (pinholes). This decoration was not observed for growth using MBE methods neither under Ga-rich or Ga-lean conditions. High-resolution reconstructions of the phase and amplitude of the complex electron exit wave showed that screw dislocations had full cores independent of the growth method. In MBE grown materials, dislocation cores appear to be stoichiometric. However, in the HVPE grown material some high intensity columns were observed within the dislocation core. Based on comparison with image calculations from model structures, it was concluded that Ga presence could be assigned to these atomic positions. Another column associated with the tip of the pyramidal void had very low intensity, suggesting the possibility of the presence of light atoms and much lower sample thickness at the void tip.

ACKNOWLEDGEMENT

This work was supported by the Director, Office of Science, Office of Basic Sciences, Material Sciences Division, of the U.S. Department of Energy under contract DE-AC03-76SF00098. The authors would like to express our gratitude to Dr. J. Northrup for sharing his models for screw dislocations with different stoichiometry; and Dr. R. Molnar for supplying HVPE grown substrates and Dr. H. Morkoc for growth of the Gan overlayers by MBE. Use of the OÅM facility at the National Center for Electron Microscopy at the LBNL is greatly appreciated.

REFERENCES:

Arslan I and Browning N D 2002 *Phys. Rev. B* **65**, 075310

Coene W M J, Thust A, Op de Beeck M and Van Dyck D 1996 *Ultramicroscopy,* **64**, 109

P. R. Elsner J, Jones R, Sitch P K, Porezag V D, Elstner M, Frauenheim T, Heggie M I, Oberg S and Briddon P R 1997 *Phys Rev Lett* **79**, 3672

Elsner J, Jones R, Sitch P K, Haugk R, Gutierrez R, Frauenheim T, Heggie M I, Oberg S and Briddon P R 1998 *Appl Phys Lett* **73**, 3530

Heying B, Wu X H, Keller S, Li Y, Kapolnek D, Keller B P, Denbaars S P and Speck J 1996 *Appl Phys Lett* **68**, 643

Hsu J W P, Manfra M J, Chu S N G, Chen C H, Pfeiffer L N and Molnar R J 2001 *Appl Phys Lett* **78**, 3980

Liliental-Weber Z, Chen Y, Ruvimov S, and Washburn J 1997a *Phys Rev Lett* **79**, 2835

Liliental-Weber Z, Washburn, Pakula K and Baranowki J 1997 b *Microscopy and Microanalysis the J. Electr. Microsc. Soc. Am*. **3**, 436

Liliental-Weber Z, D. Zakharov, J. Jasinski, M.A. O'Keefe and H. Morkoc 2003 *Microscopy and Microanalysis the J. Electr. Microsc. Soc. Am*. in print

Nakamura S. Senoh M, Nagahama S, Iwasa N, Yamada T, Matsushita T, Kiyoku H, Sugimoto Y, Kozaki T, Umemoto H, Sano M and Chocho K 1998 *Appl Phys Lett* **72**, 211

Northrup J E 2001 *Appl Phys Lett* **78**, 2288

Northrup J E 2002 *Phys Rev* **B 66**, 045204

O'Keefe M A and Kilaas R 1987 *Proc. 6th Pfefferkorn Conf. on Image and Signal Processing*, Niagara Falls, Ontario published as *Scanning Microscopy* (1988) suppl. **2** 225
O'Keefe M A, Hetherington C J D, Wang Y C, Nelson E C, Turner J H, Kisielowski C, Malm J –O, Mueller R, Ringnalda J, Pan M, and Thust A 2001 *Ultramicroscopy* **89**, 4: 215
Ponce F A, Cherns D, Young W T and Steeds J W 1996. *Appl Phys Lett* **69**, 770
Qian W, Romrer G S, Skowronski M, Doverspike K, Rowland L B and Gaskill D K 1995 *Appl Phys Lett* **67**, 2284
Thust A, Coene W M J Op De Beeck M Van Dyck D 1996 *Ultramicroscopy* **64**, 211
Trew R J, Shin M W and Gatto 1997 V Solid State Electr. **41**, 1561